ACCOUNTS of chemical research

Article

Cite This: Acc. Chem. Res. 2020, 53, 159−169

pubs.acs.org/accounts

Single-Molecule Electrical Detection: A Promising Route toward the Fundamental Limits of Chemistry and Life Science

Yu Li,[†] Chen Yang,[†] and Xuefeng Guo*

Beijing National Laboratory for Molecular Sciences, State Key Laboratory for Structural Chemistry of Unstable and Stable Species, College of Chemistry and Molecular Engineering, Peking University, Beijing 100871, P. R. China

CONSPECTUS: The ultimate limit of analytical chemistry is single-molecule detection, which allows one to visualize the dynamic processes of chemical/biological interactions with single-molecule or single-event sensitivity and hence enables the study of stochastic fluctuations under equilibrium conditions and the observation of time trajectories and reaction pathways of individual species in nonequilibrated systems. In addition, such studies may also allow the direct observation of novel microscopic quantum effects and fundamental discoveries of underlying molecular mechanisms in organic reactions and biological processes that are not accessible in ensemble experiments, thus providing unique opportunities to solve the key problems of physical, chemical, and life sciences. Consequently, the field of single-molecule detection has received considerable attention and has witnessed tremendous advances in different directions in combination with other disciplines. This Account describes our ongoing work on the development of groundbreaking methods (termed "single-molecule electrical approaches") of translating the detailed processes of chemical reactions or biological functions into detectable electrical signals at the single-event level on the platform of single-molecule electronic devices, with a particular focus on graphene−molecule−graphene single-molecule junctions (GMG-SMJs) and silicon-nanowire-based single-molecule electrical nanocircuits. These nanocircuit-based architectures are complementary to conventional optical or mechanical techniques but exhibit obvious advantages such as the absence of problems associated with bleaching and fluorescent labeling.

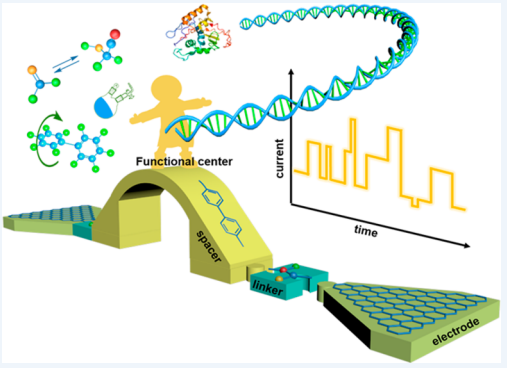

Dash-line lithography (DLL) is an efficient lithographic method of cutting graphene and forming carboxylic-acid-functionalized nanogapped graphene point contact arrays developed to address the formidable challenges of molecular device fabrication difficulty and poor stability. Molecules of interest terminated by amines on both ends can be covalently sandwiched between graphene point contacts to create high-throughput robust GMG-SMJs containing only one molecule as the conductive element. In conjunction with the ease of device fabrication and device stability, this feature distinguishes GMG-SMJs as a new testbed platform for single-molecule analysis characterized by high temporal resolution and superior signal-to-noise ratios. By exploiting the DLL method, we have fabricated molecular devices that are sensitive to external stimuli and are capable of transducing chemical/biochemical events into electrical signals at the single-molecule level, with notable examples including host−guest interaction, hydrogen bond dynamics, DNA intercalation, photoinduced conformational transition, carbocation formation, nucleophilic addition, and stereoelectronic effect. In addition to GMG-SMJs and considering compatibility with the silicon-based industry, we have also developed a reliable method of point-functionalizing silicon-nanowire-based nanotransistors to afford single-molecule electrical nanocircuits. This approach proved to be a robust platform for single-molecule electrical analysis capable of probing fast dynamic processes such as single-protein detection, DNA hybridization/polymorphism, and motor rotation dynamics.

The above systematic investigations emphasize the importance and unique advantages of universal single-molecule electrical approaches for realizing direct, label-free, real-time electrical measurements of reaction dynamics with single-event sensitivity. These approaches promise a fascinating mainstream platform to explore the dynamics of stochastic processes in chemical/biological systems as well as gain information in fields ranging from reaction chemistry for elucidating the intrinsic mechanisms to genomics or proteomics for accurate molecular and even point-of-care clinical diagnoses.

1. INTRODUCTION

The ultimate goal of analytical chemistry, namely, the detection, analysis, and manipulation of single molecules (single-molecule detection), is a rapidly developing ultrasensitive technology with adequate consideration of individual differences.[1−3] This technique allows one to directly probe heterogeneous molecular behaviors in real time during chemical and biological processes with single-molecule sensitivity and therefore uncovers a wealth of molecular information that cannot normally be accessed in conventional ensemble experiments. Consequently, single-molecule detec-

Received: June 28, 2019
Published: September 23, 2019

DOI: 10.1021/acs.accounts.9b00347
Acc. Chem. Res. 2020, 53, 159−169

tion offers crucial insights into molecular activities (i.e., kinetics and dynamics) difficult or impossible to synchronize at the ensemble level and addresses "unanswerable" questions of physical, chemical, and biological sciences. In particular, the above approaches can capture intermediates/transition states and track the time-dependent pathways of chemical reactions in organic chemistry, which is of fundamental importance for elucidating previously indecipherable intrinsic reaction mechanisms.[4,5] On the other hand, the aforementioned materials or devices can serve as local translators to sense individual binding events in biological systems (such as DNA flipping or enzymatic dynamics).[6,7] Therefore, over the past several decades, the field of single-molecule detection has witnessed significant development and substantial progress in both measurement capabilities and the fundamental understanding of diversified chemical or biological phenomena (refs 1−7 and literature cited therein).

Extensive experimental and theoretical efforts have been made to achieve efficient single-molecule detection in samples ranging in complexity from controlled in vitro conditions to the inside of living cells. Several approaches mainly based on optical and mechanical strategies such as fluorescence microscopy,[2,3,8] usage of optical tweezers,[9] fluorescence resonance energy transfer,[10] surface plasmon resonance,[11] microcavity biosensor,[10] and scanning probe microscopy (SPM)[4,12,13] have been employed to probe conformational rearrangements, enzyme activities, gene expression/regulation, chemical reactions, and molecular motions of single molecules or particles. The importance of single-molecule detection is also reflected by the fact that the 2014 Nobel Prize in Chemistry was awarded for the successful smashing of the size barrier in optical microscopy, which allowed researchers to observe individual molecules inside living cells. Although the above-mentioned methods have numerous advantages, they suffer from certain limitations; e.g., optical approaches require fluorescent labeling, which is complicated and might influence the properties of the object of interest. Moreover, the use of fluorophores poses the inevitable bleaching problem. Finally, most of these methods, such as optical and SPM approaches, feature the drawback of relatively low temporal resolution. Taken together, the presented disadvantages significantly hamper further applications of single-molecule detection in both scientific and industrial communities, which necessitates the development of an improved strategy for realizing direct, label-free, real-time electrical measurements of single molecules with high temporal/spatial resolution and high signal-to-noise ratios.

To address the above challenge, several new strategies for electrical single-molecule detection employing nanoarchitectures such as nanopores,[14] molecular junctions,[15] silicon nanowires,[16,17] organic field-effect transistors,[18] and carbon nanotubes[19,20] have been recently developed. Among these strategies, molecular junctions,[21] specifically graphene−molecule−graphene single-molecule junctions (GMG-SMJs) (Figure 1),[22] are particularly attractive as graphene is a two-dimensional carbon nanomaterial that comprises sp^2-hybridized carbon atoms arranged in a honeycomb lattice and is therefore naturally compatible with organic/biological molecules in both composition and size. The atomic stiffness, controllable morphology, superior electronic properties, and natural end-functionalities make graphene an ideal low-dimensional electrode material having the capability of covalently integrating individual molecules as the conductive

Figure 1. Schematic structure of GMG-SMJs.

channel into electrical nanocircuits to solve the key problems of fabrication difficulty and poor stability of molecular devices. Apart from that, these conceptually simple GMG-SMJs, which are built by the holistic design of electrodes, electrode/molecule contact interfaces, and functional molecular bridges,[23] covalently confine only one molecule between graphene point contacts as the conductive element, laying the foundation for single-molecule electrical detection. In combination with the advantages of device stability and ease of fabrication, this unique feature makes GMG-SMJs a robust platform for revealing and understanding the intrinsic properties of materials at the atomic- and/or molecular-length scale, reaching the ultimate limit of analytical chemistry toward the foundations of chemistry and life science. In this Account, we elaborate the development of such groundbreaking methodologies based on the use of single-molecule electrical nanocircuits, focusing on the usage of GMG-SMJs to realize direct, label-free, real-time electrical measurements of single molecules with single-event sensitivity, high signal-to-noise ratios, and high temporal resolution. A valuable survey of useful statistical analysis methods is provided, and promising future directions for the study of chemical reaction dynamics and biomolecular activities are discussed in detail, thus providing a glance at the exciting advances of this burgeoning field.

2. GRAPHENE−MOLECULE−GRAPHENE SINGLE-MOLECULE JUNCTIONS

2.1. General Fabrication Processes

Single-molecule devices are generally fabricated by integration of individual molecules of interest serving as kernel functional components into electrical circuits. Depending on the electrode materials used, molecular junctions can be classified into metal−molecule−metal SMJs (created through the fabrication of mechanically controlled break junctions, scanning tunneling microscope break junctions, conductive atomic force microscopy techniques, electromigration, on-wire lithography, and mercury drop electrode generation) and carbon nanomaterial (single-walled carbon nanotube or graphene) SMJs (refs 21 and 24 and literature cited therein). The former junctions have been used to discover remarkable new phenomena such as the Kondo effect,[25] Coulomb blockade,[26] thermoelectric effect,[27] negative differential resistance,[28] quantum interference,[29] and stereoelectronic effect,[30] which are not accessible in ensemble measurements. However, formidable challenges including gap size uncontrollability,

DOI: 10.1021/acs.accounts.9b00347
Acc. Chem. Res. 2020, 53, 159−169

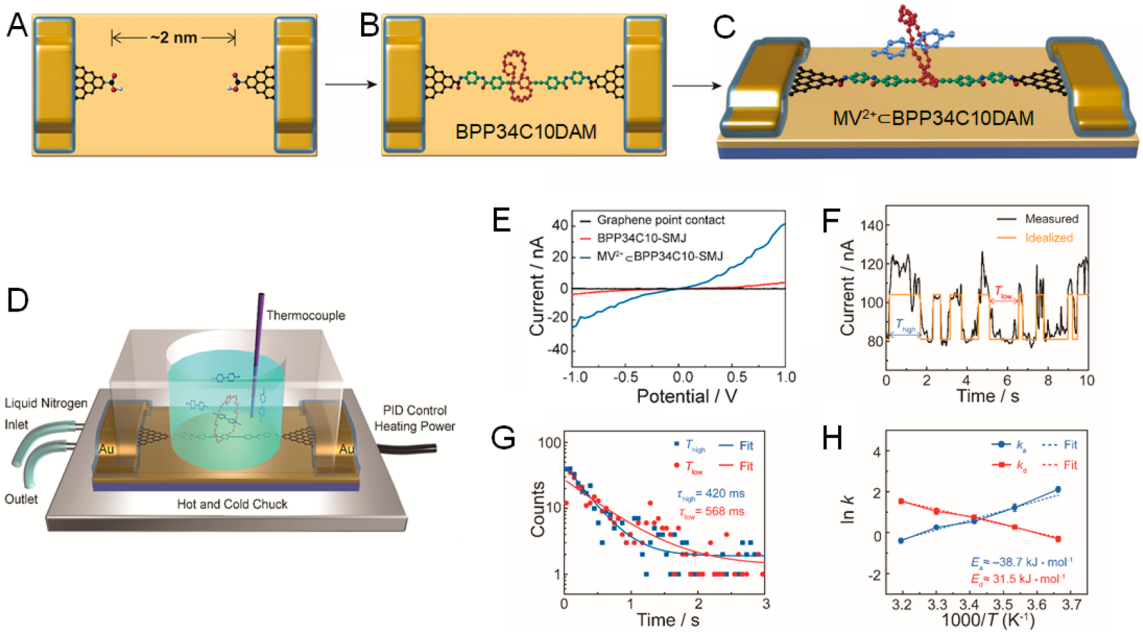

Figure 2. (A–C) Schematics of MV^{2+}⊂BPP34C10DAM GMG-SMJ device construction. (D) Schematic of the SMJ device–liquid interface characterization platform. (E) *I*–*V* curves of the device recorded at different stages. (F) *I*–*t* curve of the above device and the corresponding idealized fit obtained using QUB software. (G) Plots of time intervals of two current states for the idealized fit in (F) and corresponding Arrhenius plots (H) of association/dissociation rate constants and activation energies in Me_2SO at 293 K. V_{bias} = 100 mV.

insufficient stability, mobility of metal atoms at the nanometer scale, and the continuous mechanical breaking process of metallic junction fabrication limit the further applications of metal–molecule–metal SMJs in the investigation of fast long-term dynamics. To overcome these challenges, we focus the following discussion on the fabrication of stable GMG-SMJs.

In brief, high-quality single-layer graphene was synthesized via classical chemical vapor deposition (CVD) on copper foils. The obtained graphene films were transferred to SiO_2/Si wafers, and Au electrodes were subsequently patterned by photolithography. Nanogapped graphene point contact arrays with carboxylic acid groups on each edge were fabricated by DLL.[31] To ensure long-term in situ measurements, we constructed stable GMG-SMJs according to a bottom-up molecular assembly method and covalently linked molecules of interest terminated with amino groups on both ends to carboxylic groups at the edges of graphene point contacts via 1-ethyl-3-(3-(dimethylamino)propyl) carbodiimide coupling in pyridine. The successful formation of GMG-SMJs was confirmed by electrical current resurgence after precise etching with oxygen plasma and sequential molecular assembly. In general, conjugate molecules behave as good conducting channels, which is a prerequisite required to realize real-time monitoring of molecular dynamics. On the basis of the optimized connection yield (generally ~30.0%), statistical analysis of the binomial distribution demonstrated that the fraction of single-junction devices among the overall reconnected devices exceeds 85.8%, confirming that electron transfer mainly occurs through single-molecule junctions.

2.2. Single-Molecule Detection Based on Functional GMG-SMJs

GMG-SMJs have two salient features, namely, (i) covalent amide linkages at the molecule-electrode contact interface, which can endure chemical treatments and external stimuli and thus impart high stability, and (ii) the presence of only one molecule of interest as the local probe. The combination of these features allows one to create a new class of ultrasensitive sensors with the goal of detecting single-molecule events in solution in real time. In this section, we demonstrate the capability of electrical and long-term monitoring of in situ dynamic processes of either intermolecular interactions or chemical reactions at the single-molecule or single-event level on the GMG-SMJ platform.

2.2.1. Intermolecular Interactions. *Host–Guest Interactions.* Host–guest interactions are the basis of numerous molecular self-assembly, recognition, and biological functions. Single-molecule real-time monitoring of intermolecular host–guest interactions provides more detailed dynamic (de)-complexation information at the single-event level beyond ensemble-average measurements. To probe these interactions, we constructed a single-molecule device by covalently bridging a host molecule containing a crown ether (BPP34C10DAM) as a functional center between nanogapped graphene electrodes with amide bonds (Figure 2A and C).[32] Bias voltage-dependent current measurements confirmed the formation of GMG-SMJs (Figure 2E black and red). In the presence of the guest molecule (MV^{2+}), a new higher current level appeared (Figure 2E blue), and binary states were observed (Figure 2F), which was attributed to the dynamic interplay between host and guest molecules at the solid–liquid interface (Figure 2D). Specifically, the association of guest and host molecules (MV^{2+}⊂BPP34C10DAM) provided a more conductive channel originating from the delocalization of the molecular LUMO, which led to higher conductance. The Gaussian fits of bimodal current histograms allowed binding constants (K_a) to be derived from the Langmuir isotherm as $K_a = \alpha/(1-\alpha)C$ (α is the fraction of the BPP34C10 host complexed with MV^{2+}, and C is the concentration of MV^{2+}), while other thermodynamic parameters including the Gibbs free energy (ΔG°), enthalpy (ΔH°), and entropy (ΔS°) of complexation were deduced from the van't Hoff equation: $-RT\ \ln(K_a) =$

DOI: 10.1021/acs.accounts.9b00347
Acc. Chem. Res. 2020, 53, 159–169

$\Delta H^\circ - T\Delta S^\circ$ (R is ideal gas constant, and T is temperature). In addition to the above, I–t data for binary states were statistically fitted using QUB software (Figure 2F), and idealized two-level fluctuations were analyzed to provide a set of kinetic parameters for MV^{2+}⊂BPP34C10, including the high- and low-current-state lifetimes τ_{high} and τ_{low} (Figure 2G) and the corresponding (de)complexation rate constants $k_a = 1/\tau_{low}$ and $k_d = 1/\tau_{high}$ (Figure 2H). Finally, the Arrhenius plots of temperature-dependent ln(k) in Me_2SO demonstrated a linear dependence of ln(k) on $1/T$ (Figure 2H), and the activation energies of (de)complexation processes were obtained as $E_a = -38.7$ kJ mol^{-1} and $E_d = 31.5$ kJ mol^{-1}. These results demonstrate that the single-molecule electrical approach is sufficiently powerful to analyze and extract all thermodynamic and kinetic parameters, thus offering unlimited opportunities for probing more complex chemical/biological processes.

Hydrogen Bonding Interactions. Subsequently, we moved to explore the more complex case of hydrogen bonding interactions, which play an important role in chemical, physical, and biological processes. GMG-SMJs containing a quadrupolar hydrogen-bond dimer were constructed with two identical ureido pyrimidine-dione (UPy) molecules incorporated into the graphene point contact through amide linkages (Figure 3A).[33] The quadrupolar hydrogen-bond dimer

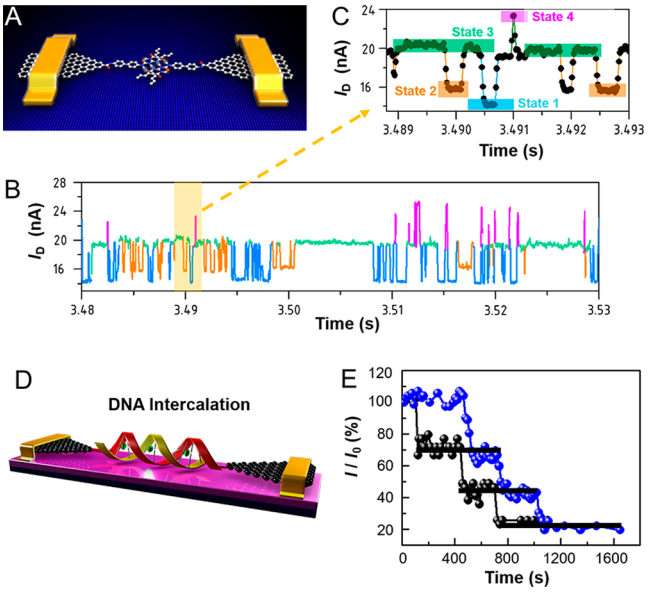

Figure 3. (A) Schematic of a quadrupolar hydrogen-bond-assembled single-molecule junction. (B, C) I–t curves recorded in diphenyl ether at different time scales and V_{bias} = 300 mV. (D) Schematics of double-stranded DNA single-molecule junctions and (E) corresponding I–t curves showing stepwise intercalation events at different EB concentrations (black, 5.0 × 10^{-7} mol L^{-1}; blue, 5.0 × 10^{-13} mol L^{-1}).

increased the strength of hydrogen bonds and device conductivity, which led to better performance and afforded more profound dynamic information in real-time electrical detection. Typically, in a weakly polar solvent such as diphenyl ether, four conductive microstates could be distinguished by real-time monitoring of junction conductance (Figure 3B and C). According to the results of theoretical calculations, the three main conductance states were assigned to the intrinsic state, the isomerized state, and the proton transfer state, respectively. Additionally, a transient weak interaction between the solvent and hydrogen bonds was suggested to afford the fourth state. Both experimental and theoretical results consistently revealed that hydrogen bonds were stochastically rearranged mainly through intermolecular proton transfer and tautomerism, confirming the possibility of intrinsically transducing an exquisite hydrogen-bond dynamic process into real-time electrical signals with single-bond resolution. In another experiment, the local distortions and unwinding of the DNA structure induced by the stepwise intercalation of ethidium bromide (EB) were monitored in real time (Figure 3D and E).[34]

2.2.2. Chemical Interaction Dynamics. As shown in previous works, minute changes in either molecular electronic or topological structure can strongly impact molecular charge transport properties. Considering this fact, we studied chemical reactions to visualize the dynamic processes of the most fundamental organic reactions at the molecular level and reveal the underlying intrinsic mechanisms.

Photoisomerization. The manipulation of molecular reactions remains a formidable challenge. To address this problem, we first chose a photoreactive diarylethene (DAE) as a functional central component. DAE is a typical photochromic molecule that can exist in the form of two (open- and closed-configuration) isomers interconverted via irradiation with UV/vis light. However, in previous works, we and others achieved only one-way photoswitching in the nanocarbon-electrode-based electrical detection platform because of the strong coupling between molecules and electrodes at the contact interface induced by covalent amide bonds.[35,36] This coupling gives rise to energy transfer between the molecular excited state and the π-electron system of carbon electrodes, which facilitates the quenching of the former and highlights the importance of the molecule–electrode contact interface, the most challenging issue that hampers the measurement of intrinsic molecular properties. To overcome this problem, we introduced three methylene (CH_2) groups on each side of the molecular backbone to weaken the molecule–electrode coupling without affecting molecular conductivity (Figure 4A)[37] and covalently sandwiched a single DAE between graphene point contacts to form a reversible molecular photoswitch. The reversible photoswitching of DAE driven by UV and visible light irradiation was confirmed by real-time electrical detection (Figure 4B). DAE open and closed states corresponded to different current levels with good stability (over a year) and an unprecedented level of accuracy (on/off ratio ≈ 100) and reproducibility, as demonstrated by the analysis of 46 different devices. Remarkably, this is the first example of a fully reversible, bimodal, single-molecule electrical switch achieved by exquisite control over matter through intellectual pursuit.

In another interesting experiment, we realized the second example of a reversible, reproducible azobenzene-based single-molecule photoswitch by making use of light- and electrical field-driven *cis*–*trans* isomerization. Specifically, an azobenzene molecular bridge was covalently incorporated between nano-gapped graphene electrodes through amide linkage formation (Figure 4C).[38] To avoid the quenching of the molecular excited state, the azobenzene moiety was introduced as the side chain of the molecular bridge, while backbone CH_2 groups were replaced by benzene rings to enhance charge transport. Both experimental and theoretical investigations demonstrated that the switching behavior could be easily detected under

DOI: 10.1021/acs.accounts.9b00347
Acc. Chem. Res. 2020, 53, 159–169

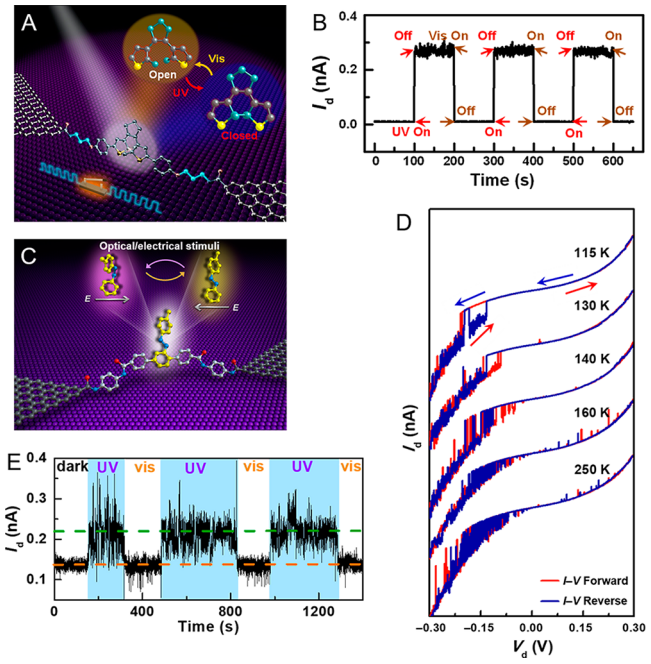

Figure 4. (A) Schematic of a single-DAE GMG-SMJ device fabricated to achieve reversible photocyclization. (B) I–t curve of the device in (A) recorded under alternate irradiation with UV and visible light. (C) Schematic of a single-azobenzene GMG-SMJ device fabricated to achieve reversible photoisomerization. (D) I–V curves of the device in (C) recorded at different temperatures and source-drain biases. (E) I–t curve of the device in (C) recorded under alternate irradiation with UV and visible light at V_{bias} = 10 mV.

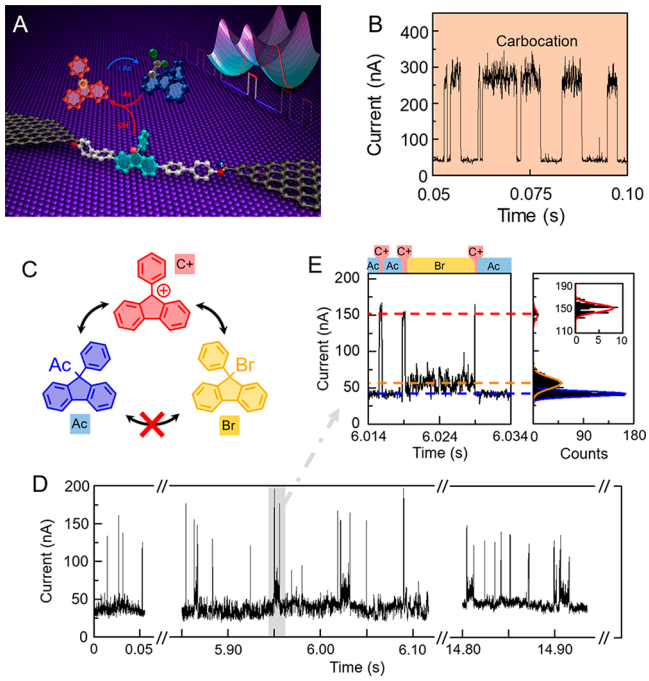

Figure 5. (A) Schematic of a single 9-phenyl-9-fluorenol-based device used to detect the S_N1 reaction. (B) I–t curve indicating carbocation formation in the presence of TFA/HAc (3:1, v/v). (C) Schematic of competitive carbocation reactions with Ac^- and Br^-. (D, E) Representative I–t trajectories and corresponding enlarged views (TFA/HAc (3:1, v/v); 10 μM Br^-). Ac, Br, and C+ represent the acetate form, the bromide form, and the carbocation form, respectively. V_{bias} = 300 mV.

different source-drain biases (Figure 4D) or at low bias voltages under alternate UV/vis light irradiation (Figure 4E) through efficient side-group chemical gating. This concept of in situ chemical gating offers a fresh perspective for creating future multifunctional single-molecule optoelectronic devices in a practical way. In addition, these results clearly demonstrate the possibility of visualizing the dynamic details of chemical reaction processes through sophisticated molecular design and engineering.

Single-Molecule Nucleophilic Substitution. To explore the capability of GMG-SMJs to detect the dynamic details of chemical reaction processes, we chose a standard nucleophilic substitution (S_N1) reaction, one of the most fundamental reactions in organic chemistry, as a proof of concept. In general, as rate-determining intermediates, carbocations have very short lifetimes and are therefore difficult to detect and manipulate. In the present work, we made use of the high temporal resolution of electrical detection (micro- or nanoseconds) to investigate an S_N1 reaction by label-free, real-time single-molecule electrical measurements.[39] A 9-phenyl-9-fluorenol functional center integrated into graphene electrodes through amide bonds (Figure 5A) underwent reversible transitions between the acetate (Ac) and carbocation forms during controlled acidity experiments (different acetic acid (HAc)/trifluoroacetic acid (TFA) ratios were used), which gave rise to repeated fluctuations between low- and high-current states in I–t plots (Figure 5B). The high-current state was ascribed to the carbocation form because of its higher extent of conjugation due to the transition of the central carbon atom from sp^3 to sp^2 hybridization, in agreement with the results of theoretical calculations. Upon the subsequent introduction of Br^-, a third state with medium conductance was observed and ascribed to the formation of the bromide form (Figure 5C and E). Interestingly, we found that all transitions from Ac to Br forms involved the formation of a high-conductance state; i.e., the competitive S_N1 reaction between acetate and bromide occurred via an inevitable carbocation intermediate (Figure 5C). After careful idealization of acidity-dependent I–t curves, we obtained the dynamic parameters of transitions between carbocation and nucleophilic substitutes, which were consistent with those obtained in ensemble experiments. Thus, these results established the reliability of the GMG-SMJ platform and demonstrated its suitability for the analysis of more complex reaction systems.

Nucleophilic Addition. In comparison with the nucleophilic substitution reaction, the nucleophilic addition reaction has a more complex mechanism, which we probed next. Previous works proved that the nucleophilic addition of NH_2OH to 9-fluorenone generally takes thousands of hours, and the final elimination product is obtained with great difficulty, which allows one to investigate the reaction mechanism without confusing the addition intermediate with the final product. As above, we incorporated 9-fluorenone between the graphene pointed electrodes using amide linkages,[40] and the carbonyl group of 9-fluorenone was reacted with NH_2OH through nucleophilic addition (Figure 6A). By monitoring the current change as a function of time, we observed distinct binary conductance states (Figure 6B and C). According to theoretical calculations, the high-current state was ascribed to 9-fluorenone, while the low-current state was attributed to the addition intermediate. The decrease of current upon

DOI: 10.1021/acs.accounts.9b00347
Acc. Chem. Res. 2020, 53, 159–169

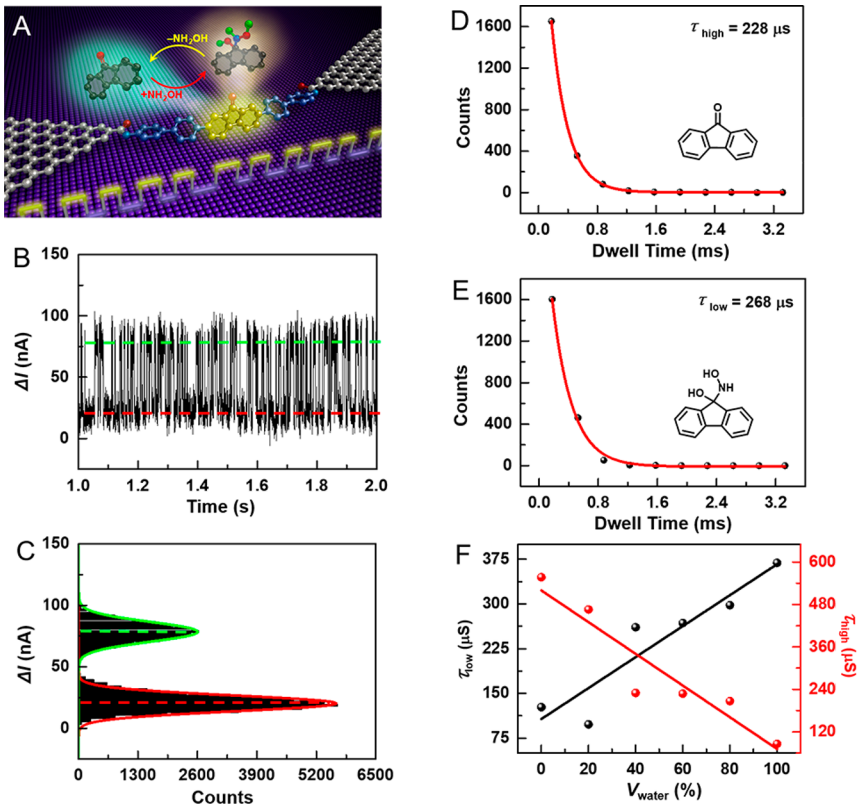

Figure 6. (A) Schematic of a single 9-fluorenone-molecule-based device used to detect the nucleophilic addition reaction. (B, C) *I*−*t* curve and corresponding histogram of current values showing a distinct bimodal current distribution. V_{bias} = 300 mV. (D, E) Plots of time intervals used to determine the lifetimes of each state (intermediate, τ_{low}; substrate, τ_{high}) (60% water in EtOH at 298 K). (F) Lifetimes of the low-current (intermediate: black) and high-current (substrate: red) states as functions of water content.

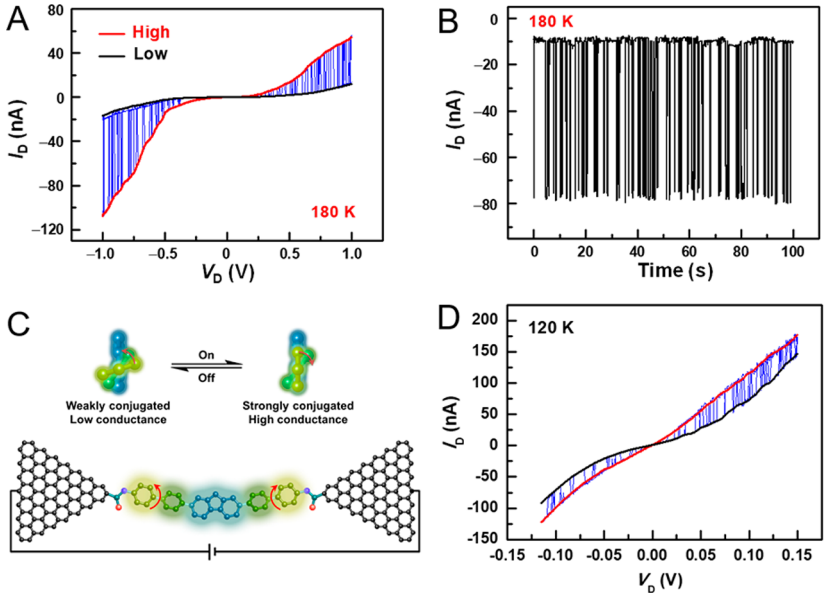

Figure 7. (A) Stochastic switching between two conductive states of individual closed DAEs at 180 K. (B) Corresponding real-time recording of stochastic conductance switching at 180 K. V_{bias} = −800 mV. (C) Schematic of a single-molecule hexaphenyl aromatic device. (D) *I*−*V* curves of the device in (C) recorded at 120 K and showing similar stochastic switching.

nucleophilic addition was rationalized by the concomitant transition of the central carbon atom from sp^2 to sp^3 hybridization (opposite to the carbocation case) and demonstrated the successful capture of a new addition intermediate, as predicted. Furthermore, we used solvent polarity-dependent experiments to systematically analyze the dwell times of the substrate (τ_{high}) and the intermediate (τ_{low}) (Figure 6D and E), revealing that the intermediate stability increased with solvent polarity, as the intermediate was more polar than the substrate. Correspondingly, with increasing the

DOI: 10.1021/acs.accounts.9b00347
Acc. Chem. Res. 2020, 53, 159−169

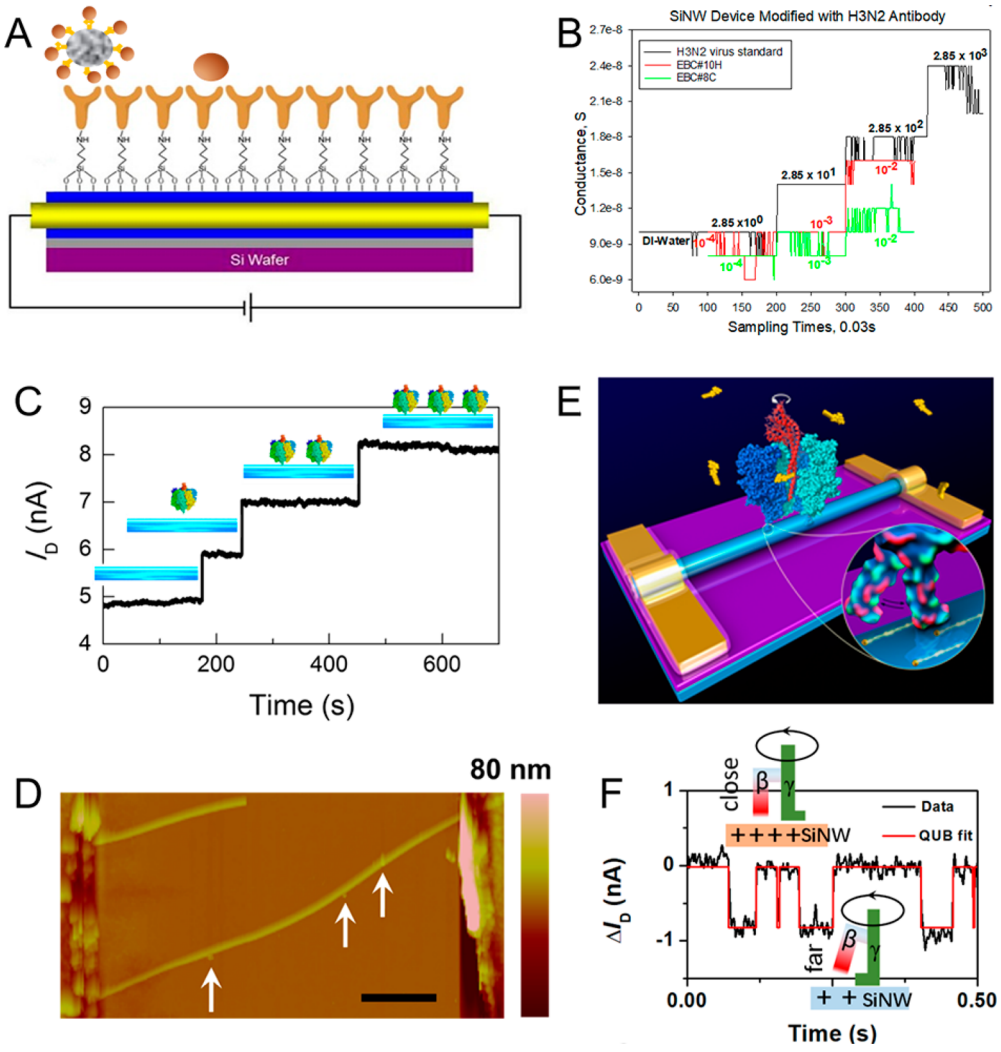

Figure 8. (A) Antibody-modified SiNW-FET-based sensors for influenza virus detection. (B) Detection of H3N2 viruses at different concentrations in 100-fold-diluted EBC samples. (C, D) Real-time recordings of absorption/desorption of F_1-ATPases and corresponding AFM images. (E, F) Schematics of a single-F_1-molecule-modified SiNW-FET nanocircuit and statistical analysis of F_1 hydrolysis. Insets in (F) show different β conformations corresponding to high- and low-conductance states.

solvent polarity, the equilibrium position shifted to the side of the intermediate (Figure 6F), in agreement with the results of ensemble experiments. Thus, this study presents a powerful and elegant combination of molecular electronics, quantum chemistry, and single-molecule chemical physics, providing a textbook-like clarity.

Stereoelectronics. The essence of a chemical reaction is the vibrational rupture and generation of chemical bonds between atoms. Therefore, the different vibration states of a molecule should inevitably impact the dynamics of a chemical reaction. Vibration or rotation of functional groups could cause changes in molecular conjugation and thus the electronic structure. We are curious about whether these tiny changes lead to different conductivities.[30,41] By exploiting the good stability of the GMG-SMJ electrical detection platform, we have previously established a reversible bimodal single-molecule photoswitch based on individual DAEs. Notably, reproducible stochastic switching of the closed junction between two conductive modes was observed in a DAE system during systematical measurements at low temperatures, as demonstrated by $I-V$ (Figure 7A) and $I-t$ (Figure 7B) curves. This surprising finding was attributed to a DAE conformational change such as rotation around the σ bond between thiophene and benzene rings in the closed DAE form. Inspired by this hypothesis, we investigated stereoelectronic effects in a specifically designed hexaphenyl aromatic chain, where the central biphenyl was introduced in a fluorene form to fix the dihedral angle. In a similar approach, an amine-terminated hexaphenyl aromatic chain was sandwiched between carboxylic-acid-terminated graphene electrodes to disclose single-molecule charge transport properties (Figure 7C).[42] In temperature-dependence experiments, we did observe a similar stochastic switching of conductance in the temperature range of 120−140 K (Figure 7D). According to theoretical calculations, this stochastic switching originated from rotation around the σ bond between biphenyl rings to alternately form strongly and weakly conjugated states, which proved the correctness of the above hypothesis. Thus, the switching of conductance originated from a typical stereoelectronic effect that is ubiquitous in organic chemistry, which offered a fresh perspective for revealing structure−property relationships and constructing future functional molecular electronic devices on the sophisticated platform of GMG-SMJs.

DOI: 10.1021/acs.accounts.9b00347
Acc. Chem. Res. 2020, 53, 159−169

3. SINGLE-MOLECULE ELECTRICAL DETECTION BASED ON SILICON-NANOWIRE-BASED NANOCIRCUITS

As the Si/SiO_2 interface is the basis for the prosperity of today's mainstream microelectronics, it is natural that one-dimensional silicon nanowires (1D SiNWs) have attracted much attention as basic nanobuilding blocks.[43,44] SiNWs exhibit the unique advantages of high biocompatibility, size comparability, capability of integration with the existing silicon industry, and flexible surface tailorability, while their easy availability through bottom-up approaches and superior electrical properties with precise controllability make SiNWs well suited for the fabrication of high-gain field-effect transistors (FETs) whose conductance is highly dependent on the local charge density.[45,46] The above merits allow SiNW-FETs to be intimately interfaced with biological circuits at different scales ranging from individual molecules to animal organs. In this section, we demonstrate the capability of SiNW-FETs to sense individual biomolecules or probe the dynamic processes of biological systems.

3.1. Surface Functionalization: Single-Protein Detection

Rapid, selective, and sensitive detection of viruses is an effective tool for the diagnosis of viral infections. Previous studies reported highly selective SiNW-FETs as a promising platform for ultrasensitive virus detection.[16] For a practical attempt, we modified the surface of SiNW sensors with antibodies to detect influenza viruses H3N2 and H1N1 that were collected from clinical exhaled breathe condensates (EBCs) of patients with and without flu symptoms (Figure 8A).[47] As a result, the SiNW biosensors could selectively detect influenza A viruses within minutes at levels as low as ~285 viruses/μL in 100-fold diluted flu EBC samples (Figure 8B) and thus distinguish them from non-flu EBC samples (~29 viruses/μL). This method considerably extends the scope of SiNW sensing to the diagnosis of flu in clinical settings and is 2 orders of magnitude faster than the gold standard method of RT-qPCR.

In another work, single-protein detection was realized by surface functionalization before SiNW transfer to build a SiNW-FET-based biosensor capable of directly detecting protein adsorption/desorption at the single-event level, where the biomolecules of interest act as a local gate after assembly and electrostatically modulate the carrier intensity inside the nanowires.[48,49] Specifically, Ni-NTA end groups (Ni^{2+} chelated Nα,Nα-bis(carboxymethyl)-L-lysine hydrate) serving as selective binding sites for His-tag F_1-ATPase (F_1) immobilization were used, and the stepwise adsorption of individual F_1 molecules was monitored by real-time electrical detection (Figure 8C) and atomic force microscopy (AFM) (Figure 8D). This approach was used to fabricate single-F_1-molecule-grafted SiNW-FETs that displayed steady conductance in buffer solution.[49] Interestingly, the introduction of ATP resulted in a reproducible two-level current fluctuation, which originated from the biconformational transition of the γ shaft of F_1 corresponding to ATP hydrolysis and Pi release (Figure 8E and F), respectively. Importantly, the rate of label-free F_1 hydrolysis obtained in this work was 1 order of magnitude higher (1.69×10^8 M^{-1} s^{-1} at 20 °C) than that in the case of fluorescent tag-labeled F_1, which manifested the capability of SiNW-based electrical nanocircuits to non-destructively probe the intrinsic dynamics of biological activities.

3.2. Point Functionalization: DNA Hybridization and Polymorphism

A particularly interesting feature of CVD-grown SiNWs is their 1D Si/SiO_2 core–shell structure,[50] which allows one to open functional nanogaps for subsequent biocompatible assembly. Taking advantages of this feature, we developed a reliable method of point functionalization with precise high-resolution electron-beam lithography, which is able to open a ~ 10 nm window in the spin-cast poly(methyl methacrylate) layer (Figure 9A and B). This process produced a H-terminated Si surface perpendicular to SiNWs for programmed point decoration assembly and subsequent detection of single proteins in combination with microfluidics.[51] Remarkably, at very low protein concentrations (7.8 to 78 and 780 pg/mL), in situ electrical measurements showed no concentration dependence, thus demonstrating single-molecule sensitivity (Figure 9C).

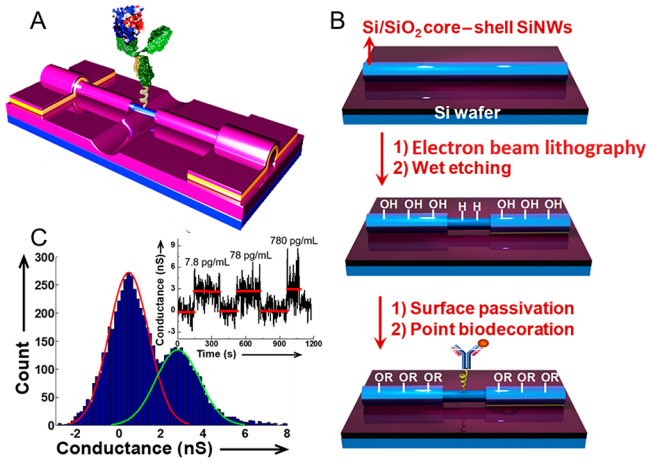

Figure 9. (A) Device structure of single-molecule biosensors formed by point decoration of SiNWs. (B) Three-step process used to fabricate SiNW-FET-based single-molecule electrical biosensors. (C) Conductance histograms recorded in deionized water (red line) and antigen solution (green line). Inset shows the results of corresponding in situ electrical measurements. V_{bias} = 50 mV.

DNA hybridization/polymorphism is a fundamental process in biology, with the DNA hairpin-loop being a classical folding/unfolding system for DNA hybridization studies. With the development of optical detection techniques, the generally adopted mechanism of DNA hybridization has gradually changed from the initially proposed two-state model to the multistate model.[52] However, accurate information on each stage of hybridization is still lacking. To bridge this gap, we tethered individual hairpin DNAs on SiNWs through active ester terminals on the platform of SiNW-FET-based single-molecule biosensors described above (Figure 10A and B)[17] and observed multiple-step current changes during DNA hybridization dynamic measurements, which were performed at precisely controlled temperatures of 20–65 °C (temperature increase step = 5 °C) (Figure 10C). This observation agreed with the number of base pairs in the stem of hairpin DNAs, thus clearly demonstrating the single-base resolution of the DNA folding/unfolding processes within a time scale of a few milliseconds (Figure 10D). As a further step toward real-life applications, we utilized a molecular hairpin DNA probe to establish a low-cost, high-throughput, simple, and accurate single-nucleotide polymorphism genotyping technique.[53]

DOI: 10.1021/acs.accounts.9b00347
Acc. Chem. Res. 2020, 53, 159–169

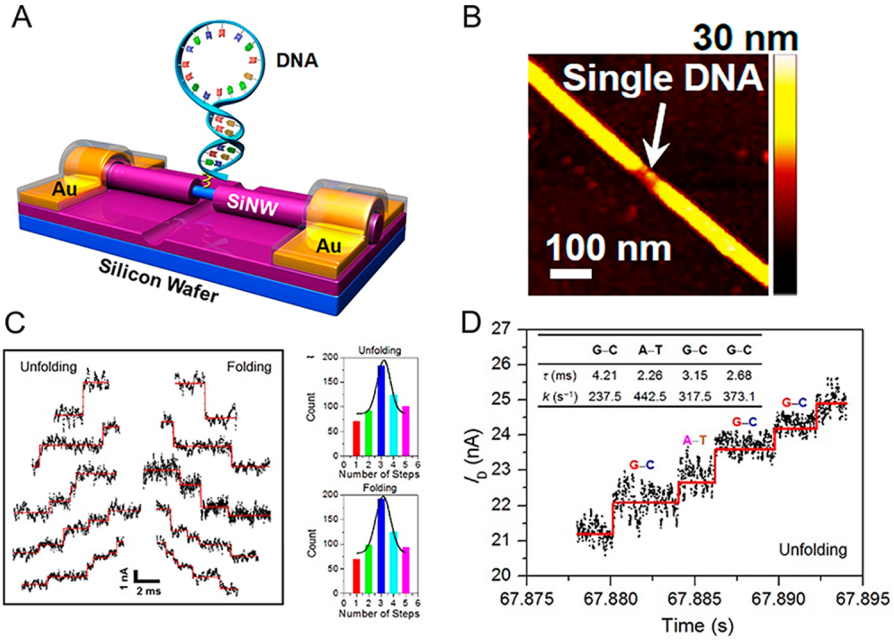

Figure 10. (A, B) Schematic diagram of a single-hairpin DNA-decorated SiNW biosensor and corresponding AFM image. (C) Stepwise folding/unfolding processes fitted by a step-finding algorithm (red), showing zero- to five-step changes, and corresponding histograms of step numbers in unfolding and folding data counted from thousands of current oscillating events. (D) Representative five-step unfolding data. Inset shows the kinetic parameters of each plateau (lifetime τ and rate constant k).

Collectively, the above investigations prove that SiNW-FET single-molecule electrical circuits offer a powerful platform for researchers to study fast single-molecule biophysics in an interdisciplinary realm and can be used in numerous applications such as genetic polymorphism, protein folding, enzymatic activity, and reaction mechanism elucidation.

4. CONCLUSIONS AND PERSPECTIVES

In this Account, we present two types of sophisticated and universal methodologies based on the reliable platforms of GMG-SMJs or SiNW-FET single-molecule electrical nanocircuits, which have the capability of achieving direct, label-free, real-time electrical measurements of the single-molecule dynamic processes of chemical/biological events in in situ environments, thus opening up a new direction in the field of single-molecule science and technology. From the development of proof-of-principle strategies to the application of single-molecule detection, we demonstrate the powerful ability of these methodologies to disclose a wealth of kinetic and thermodynamic molecular information that synchronizes the molecular activities in both chemical reactions (such as host–guest interactions, hydrogen bond dynamics, photoinduced conformational transitions, carbocation formation, nucleophilic addition, and stereoelectronics) and biological functions (such as single-protein detection, motor rotation dynamics, and DNA hybridization/polymorphism). Considering the overwhelming degree of material diversity and functionality with exquisite control over molecular design through chemical synthesis and the abundance of room at the fundamental limits of chemistry and life science, the proven device stability, the maturity of the device fabrication procedure, and the ability to reach the ultimate limit of analytical chemistry offer infinite opportunities to elucidate the fundamental mechanisms of chemical reactions and uncover important details of the most basic processes of life. The global scientific benefit is the establishment of a mainstream approach to study single-molecule/single-event physics in an interdisciplinary realm, which is expected to revolutionize single-molecule analysis from static to dynamic, from qualitative to quantitative, and from monodisciplinary to multidisciplinary. In addition to scientific contributions, these methodologies build a foundation for creating robust, versatile, universally available, low-cost, and accurate tools for molecular or even point-of-care clinical diagnostics. Such novel single-molecule biosensors also offer a new solution urgently needed for high-efficiency genetic testing.

■ AUTHOR INFORMATION

Corresponding Author

*E-mail: guoxf@pku.edu.cn (X.G.).

ORCID

Xuefeng Guo: 0000-0001-5723-8528

Author Contributions

†Y.L. and C.Y. contributed equally to the work.

Funding

We acknowledge primary financial supports from National Key R&D Program of China (2017YFA0204901), NSFC (21727806 and 21933001), and NSFB (Z181100004418003).

Notes

The authors declare no competing financial interest.

Biographies

Yu Li received her Ph.D. from Tokyo Institute of Technology in 2017 and started to work as a postdoc. with Prof. Xuefeng Guo in College of Chemistry and Molecular Engineering (CCME), Peking University. Her research interest includes single-molecule device physics and biophysics.

Chen Yang received his B.S. degree from Lanzhou University in 2017. Now, he is a Ph.D. candidate in CCME, Peking University, under the

DOI: 10.1021/acs.accounts.9b00347
Acc. Chem. Res. 2020, 53, 159−169

guidance of Prof. Xuefeng Guo. His current research interests concentrate on single-molecule dynamics.

Xuefeng Guo received his Ph.D. in 2004 from the Institute of Chemistry, Chinese Academy of Sciences, Beijing. From 2004 to 2007, he was a postdoc at the Columbia University Nanocenter. He joined the faculty as a professor under "Peking 100-Talent" Program at Peking University in 2008. His current research is focused on functional nanometer/molecular devices.

REFERENCES

(1) Walter, N.; Huang, C.; Manzo, A.; Sobhy, M. Do-it-yourself guide: How to use the modern single-molecule toolkit. *Nat. Methods* **2008**, *5*, 475−478.

(2) Wang, C.; Bai, C. *Single molecule chemistry and physics: An introduction*; Springer Science & Business Media, 2006.

(3) Kulzer, F.; Orrit, M. Single-molecule optics. *Annu. Rev. Phys. Chem.* **2004**, *55*, 585−611.

(4) Hla, S. W.; Rieder, K. H. STM control of chemical reactions: Single-molecule synthesis. *Annu. Rev. Phys. Chem.* **2003**, *54*, 307−330.

(5) Polanyi, J. C.; Zewail, A. H. Direct observation of the transition state. *Acc. Chem. Res.* **1995**, *28*, 119−132.

(6) Yin, Y.; Yang, L.; Zheng, G.; Gu, C.; Yi, C.; He, C.; Gao, Y. Q.; Zhao, X. S. Dynamics of spontaneous flipping of a mismatched base in DNA duplex. *Proc. Natl. Acad. Sci. U. S. A.* **2014**, *111*, 8043−8048.

(7) Lu, H.; Xun, L.; Xie, X. Single-molecule enzymatic dynamics. *Science* **1998**, *282*, 1877−1882.

(8) Zhuang, X.; Bartley, L. E.; Babcock, H. P.; Russell, R.; Ha, T.; Herschlag, D.; Chu, S. A single-molecule study of RNA catalysis and folding. *Science* **2000**, *288*, 2048−2051.

(9) Bustamante, C.; Bryant, Z.; Smith, S. B. Ten years of tension: Single-molecule DNA mechanics. *Nature* **2003**, *421*, 423−427.

(10) Baaske, M.; Foreman, M.; Vollmer, F. Single-molecule nucleic acid interactions monitored on a label-free microcavity biosensor platform. *Nat. Nanotechnol.* **2014**, *9*, 933−939.

(11) Halpern, A.; Wood, J.; Wang, Y.; Corn, R. Single-nanoparticle near-infrared surface plasmon resonance microscopy for real-time measurements of DNA hybridization adsorption. *ACS Nano* **2014**, *8*, 1022−1030.

(12) Hansma, H.; Kasuya, K.; Oroudjev, E. Atomic force microscopy imaging and pulling of nucleic acids. *Curr. Opin. Struct. Biol.* **2004**, *14*, 380−385.

(13) Uchihashi, T.; Iino, R.; Ando, T.; Noji, H. High-speed atomic force microscopy reveals rotary catalysis of rotorless F_1-ATPase. *Science* **2011**, *333*, 755−758.

(14) Howorka, S.; Siwy, Z. Nanopore analytics: Sensing of single molecules. *Chem. Soc. Rev.* **2009**, *38*, 2360−2384.

(15) Zhao, Y.; Ashcroft, B.; Zhang, P.; Liu, H.; Sen, S.; Song, W.; Im, J.; Gyarfas, B.; Manna, S.; Biswas, S.; Borges, C.; Lindsay, S. Single-molecule spectroscopy of amino acids and peptides by recognition tunnelling. *Nat. Nanotechnol.* **2014**, *9*, 466−473.

(16) Patolsky, F.; Zheng, G.; Hayden, O.; Lakadamyali, M.; Zhuang, X.; Lieber, C. M. Electrical detection of single viruses. *Proc. Natl. Acad. Sci. U. S. A.* **2004**, *101*, 14017−14022.

(17) He, G.; Li, J.; Ci, H.; Qi, C.; Guo, X. Direct measurement of single-molecule DNA hybridization dynamics with single-base resolution. *Angew. Chem. Int. Ed.* **2016**, *55*, 9036−9040.

(18) Macchia, E.; Manoli, K.; Holzer, B.; Di Franco, C.; Ghittorelli, M.; Torricelli, F.; Alberga, D.; Mangiatordi, G. F.; Palazzo, G.; Scamarcio, G.; et al. Single-molecule detection with a millimetre-sized transistor. *Nat. Commun.* **2018**, *9*, 3223.

(19) Choi, Y.; Moody, I.; Sims, P.; Hunt, S.; Corso, B.; Perez, I.; Weiss, G. A.; Collins, P. G. Single-molecule lysozyme dynamics monitored by an electronic circuit. *Science* **2012**, *335*, 319−324.

(20) Guo, X.; Small, J. P.; Klare, J. E.; Wang, Y.; Purewal, M. S.; Tam, I. W.; Hong, B. H.; Caldwell, R.; Huang, L.; O'brien, S.; et al. Covalently bridging gaps in single-walled carbon nanotubes with conducting molecules. *Science* **2006**, *311*, 356−359.

(21) Xiang, D.; Wang, X.; Jia, C.; Lee, T.; Guo, X. Molecular-scale electronics: from concept to function. *Chem. Rev.* **2016**, *116*, 4318−4440.

(22) Jia, C.; Ma, B.; Xin, N.; Guo, X. Carbon electrode-molecule junctions: A reliable platform for molecular electronics. *Acc. Chem. Res.* **2015**, *48*, 2565−2575.

(23) Xin, N.; Guan, J.; Zhou, C.; Chen, X.; Gu, C.; Li, Y.; Ratner, M. A.; Nitzan, A.; Stoddart, J.; Guo, X. Concepts in the design and engineering of single-molecule electronic devices. *Nat. Rev. Phys.* **2019**, *1*, 211−230.

(24) Elke, S.; Carlos, C. J. *Molecular electronics: An introduction to theory and experiment*; World Scientific, 2017; Vol. *15*.

(25) Calvo, M.; Fernandez-Rossier, J.; Palacios, J.; Jacob, D.; Natelson, D.; Untiedt, C. The Kondo effect in ferromagnetic atomic contacts. *Nature* **2009**, *458*, 1150−1153.

(26) Park, J.; Pasupathy, A.; Goldsmith, J.; Chang, C.; Yaish, Y.; Petta, J.; Rinkoski, M.; Sethna, J.; Abruña, H.; McEuen, P.; et al. Coulomb blockade and the Kondo effect in single-atom transistors. *Nature* **2002**, *417*, 722−725.

(27) Aradhya, S. V.; Venkataraman, L. Single-molecule junctions beyond electronic transport. *Nat. Nanotechnol.* **2013**, *8*, 399−410.

(28) Chen, J.; Reed, M.; Rawlett, A.; Tour, J. Large on-off ratios and negative differential resistance in a molecular electronic device. *Science* **1999**, *286*, 1550−1552.

(29) Wu, S.; González, M. T.; Huber, R.; Grunder, S.; Mayor, M.; Schönenberger, C.; Calame, M. Molecular junctions based on aromatic coupling. *Nat. Nanotechnol.* **2008**, *3*, 569−574.

(30) Su, T.; Li, H.; Steigerwald, M.; Venkataraman, L.; Nuckolls, C. Stereoelectronic switching in single-molecule junctions. *Nat. Chem.* **2015**, *7*, 215−220.

(31) Cao, Y.; Dong, S.; Liu, S.; He, L.; Gan, L.; Yu, X.; Steigerwald, M. L.; Wu, X.; Liu, Z.; Guo, X. Building high-throughput molecular junctions using indented graphene point contacts. *Angew. Chem. Int. Ed.* **2012**, *51*, 12228−12232.

(32) Wen, H.; Li, W.; Chen, J.; He, G.; Li, L. H.; Olson, M.; Sue, A.; Stoddart, J.; Guo, X. Complex formation dynamics in a single-molecule electronic device. *Sci. Adv.* **2016**, *2*, No. e1601113.

(33) Zhou, C.; Li, X.; Gong, Z.; Jia, C.; Lin, Y.; Gu, C.; He, G.; Zhong, Y.; Yang, J.; Guo, X. Direct observation of single-molecule hydrogen-bond dynamics with single-bond resolution. *Nat. Commun.* **2018**, *9*, 807.

(34) Wang, X.; Gao, L.; Liang, B.; Li, X.; Guo, X. Revealing the direct effect of individual intercalations on DNA conductance toward single-molecule electrical biodetection. *J. Mater. Chem. B* **2015**, *3*, 5150−5154.

(35) Whalley, A. C.; Steigerwald, M. L.; Guo, X.; Nuckolls, C. Reversible switching in molecular electronic devices. *J. Am. Chem. Soc.* **2007**, *129*, 12590−12591.

(36) Dulić, D.; van der Molen, S. J.; Kudernac, T.; Jonkman, H. T.; de Jong, J. J.; Bowden, T. N.; van Esch, J.; Feringa, B. L.; van Wees, B. J. One-way optoelectronic switching of photochromic molecules on gold. *Phys. Rev. Lett.* **2003**, *91*, 207402.

(37) Jia, C.; Migliore, A.; Xin, N.; Huang, S.; Wang, J.; Yang, Q.; Wang, S.; Chen, H.; Wang, D.; Feng, B.; Liu, Z.; Zhang, G.; Qu, D.; Tian, H.; Ratner, M.; Xu, H.; Nitzan, A.; Guo, X. Covalently bonded single-molecule junctions with stable and reversible photoswitched conductivity. *Science* **2016**, *352*, 1443−1445.

(38) Meng, L.; Xin, N.; Hu, C.; Wang, J.; Gui, B.; Shi, J.; Wang, C.; Shen, C.; Zhang, G.; Guo, H.; Meng, S.; Guo, X. Side-group chemical gating via reversible optical and electric control in a single molecule transistor. *Nat. Commun.* **2019**, *10*, 1450.

(39) Gu, C.; Hu, C.; Wei, Y.; Lin, D.; Jia, C.; Li, M.; Su, D.; Guan, J.; Xia, A.; Xie, L.; Nitzan, A.; Guo, H.; Guo, X. Label-free dynamic detection of single-molecule nucleophilic-dubstitution teactions. *Nano Lett.* **2018**, *18*, 4156−4162.

(40) Guan, J. X.; Jia, C. C.; Li, Y. W.; Liu, Z. T.; Wang, J. Y.; Yang, Z. Y.; Gu, C. H.; Su, D. K.; Houk, K. N.; Zhang, D. Q.; Guo, X. Direct single-molecule dynamic detection of chemical reactions. *Sci. Adv.* **2018**, *4*, No. eaar2177.

DOI: 10.1021/acs.accounts.9b00347
Acc. Chem. Res. 2020, 53, 159−169

(41) Venkataraman, L.; Klare, J. E.; Nuckolls, C.; Hybertsen, M. S.; Steigerwald, M. L. Dependence of single-molecule junction conductance on molecular conformation. *Nature* **2006**, *442*, 904−907.
(42) Xin, N.; Wang, J.; Jia, C.; Liu, Z.; Zhang, X.; Yu, C.; Li, M.; Wang, S.; Gong, Y.; Sun, H.; Zhang, G.; Liu, Z.; Zhang, G.; Liao, J.; Zhang, D.; Guo, X. Stereoelectronic effect-induced conductance switching in aromatic chain single-molecule junctions. *Nano Lett.* **2017**, *17*, 856−861.
(43) Dai, X.; Hong, G.; Gao, T.; Lieber, C. M. Mesh nanoelectronics: Seamless integration of electronics with tissues. *Acc. Chem. Res.* **2018**, *51*, 309−318.
(44) Liu, S.; Shen, Q.; Cao, Y.; Gan, L.; Wang, Z.; Steigerwald, M. L.; Guo, X. Chemical functionalization of single-walled carbon nanotube field-effect transistors as switches and sensors. *Coord. Chem. Rev.* **2010**, *254*, 1101−1116.
(45) Jiang, Y. W.; Tian, B. Z. Inorganic semiconductor biointerfaces. *Nat. Rev. Mater.* **2018**, *3*, 473−490.
(46) Stern, E.; Klemic, J.; Routenberg, D.; Wyrembak, P.; Turner-Evans, D.; Hamilton, A.; LaVan, D.; Fahmy, T.; Reed, M. Label-free immunodetection with CMOS-compatible semiconducting nanowires. *Nature* **2007**, *445*, 519−522.
(47) Shen, F.; Wang, J.; Xu, Z.; Wu, Y.; Chen, Q.; Li, X.; Jie, X.; Li, L.; Yao, M.; Guo, X.; et al. Rapid flu diagnosis using silicon nanowire sensor. *Nano Lett.* **2012**, *12*, 3722−3730.
(48) Li, J.; He, G.; Ueno, H.; Jia, C.; Noji, H.; Qi, C.; Guo, X. Direct real-time detection of single proteins using silicon nanowire-based electrical circuits. *Nanoscale* **2016**, *8*, 16172−16176.
(49) Li, J.; He, G.; Hiroshi, U.; Liu, W.; Noji, H.; Qi, C.; Guo, X. Direct measurement of single-molecule adenosine triphosphatase hydrolysis dynamics. *ACS Nano* **2017**, *11*, 12789−12795.
(50) Cui, Y.; Zhong, Z.; Wang, D.; Wang, W. U.; Lieber, C. High performance silicon nanowire field effect transistors. *Nano Lett.* **2003**, *3*, 149−152.
(51) Wang, J.; Shen, F.; Wang, Z.; He, G.; Qin, J.; Cheng, N.; Yao, M.; Li, L.; Guo, X. Point decoration of silicon nanowires: An approach toward single-molecule electrical detection. *Angew. Chem. Int. Ed.* **2014**, *53*, 5038−5043.
(52) Yin, Y.; Zhao, X. Kinetics and dynamics of DNA hybridization. *Acc. Chem. Res.* **2011**, *44*, 1172−1181.
(53) He, G.; Li, J.; Qi, C.; Guo, X. Single nucleotide polymorphism genotyping in single-molecule electronic circuits. *Adv. Sci.* **2017**, *4*, 1700158.

DOI: 10.1021/acs.accounts.9b00347
Acc. Chem. Res. 2020, 53, 159−169